



ORIGINAL ARTICLE

The structural and optical properties of ZnO thin films prepared at different RF sputtering power

A. Ismail *, M.J. Abdullah

School of Physics, Universiti Sains Malaysia, 11800 Penang, Malaysia

Received 23 September 2012; accepted 16 December 2012

Available online 27 December 2012

KEYWORDS

Zinc oxide;
Optical properties;
X-ray diffraction;
Photoluminescence and
Raman spectra

Abstract ZnO thin films were prepared on glass and Si(100) substrates by RF sputtering. The thickness, crystallinity, and the optical properties of the films were observed to vary with the RF power used. All the films exhibited preferred *c*-axis oriented (002) phase of wurtzite structure. The values of *d*-spacing for ZnO films were higher than those of the *d*-spacing for ZnO powder, suggesting that all the ZnO films experienced tensile strain. Good optical transmittance of 70–88% in the visible range has been observed in all the films. The PL spectra showed a dominant UV emission peak that shifted from 3.31 eV to 3.17 eV with decreasing RF power of the sample. The Raman lines around 433.26 cm⁻¹ and 573.72 cm⁻¹ attributed to *E*₂ (high) and *A*₁ (LO) respectively, were observed for all the ZnO films. The presence of tensile strain in the ZnO films was evident from the results of Raman spectra and XRD data. Defects due to oxygen vacancy in the prepared ZnO films were manifested in the PL and Raman spectra characteristics.

© 2013 King Saud University. Production and hosting by Elsevier B.V. All rights reserved.

1. Introduction

ZnO is well-known for various applications, such as varistors, gas sensors and transparent conductors for thin film transistors and solar cells. The other emerging applications include light emitting diodes (LEDs), laser diodes (LDs) and light detectors. These applications are attributed to the interesting material properties of a wide and direct band gap (3.37 eV) and high exciton binding energy (60 meV). The rich in defects is another important characteristic that has a

direct impact on the electrical and optical properties of the material (Ozgun et al., 2005; Lau et al., 2005; Alivov et al., 2003; Chen et al., 2011; Singh et al., 2012; Sun et al., 2011; Qiao et al., 2012).

ZnO thin films can be prepared by techniques such as thermal oxidation (Rusu et al., 2007), chemical vapor deposition (Li et al., 2002), molecular beam epitaxy (Ohgaki et al., 2003) and pulsed laser deposition (Ryu and Zhu, 2000). The technique of RF sputtering has drawn considerable attention for ZnO film fabrication since the resulting film properties can be controlled by changing the sputtering conditions such as substrate temperature, deposition time, pressure, and RF power. However, the effect of changing the RF power on the ZnO film properties has not been much reported in the literature.

In this work, ZnO thin films were deposited by RF sputtering on Si(100) and glass substrates. The effect of the change in

* Corresponding author. Tel.: +60 175272166; fax: +60 46579150.
E-mail address: aia09_phy083@student.usm.my (A. Ismail).

Peer review under responsibility of King Saud University.



Production and hosting by Elsevier

the RF power on the structural and optical properties of ZnO thin films was investigated.

2. Experimental

ZnO films were deposited by RF sputtering using high purity ZnO target of 7.6 cm diameter. The substrates used were *n*-type Si with (100) orientation and microscope slide glass. The substrates were initially cleaned with acetone and isopropanol in an ultrasonic bath for 15 min and rinsed with deionized water, before being fixed to a rotating substrate holder of the Edwards A500 RF sputtering unit at a distance of 10 cm above the ZnO target. Mechanical rotary pump and turbo pump were used to evacuate the sputtering chamber to its ultimate pressure of about 5×10^{-5} mbar. Argon (Ar) of high purity (99.99%) was used as sputtering gas. The pressure inside the chamber was maintained at 2×10^{-2} mbar during the sputtering process. The ZnO films were deposited at different RF powers of 150 W, 175 W, 200 W, 225 W and 250 W for 50 min for each of the samples.

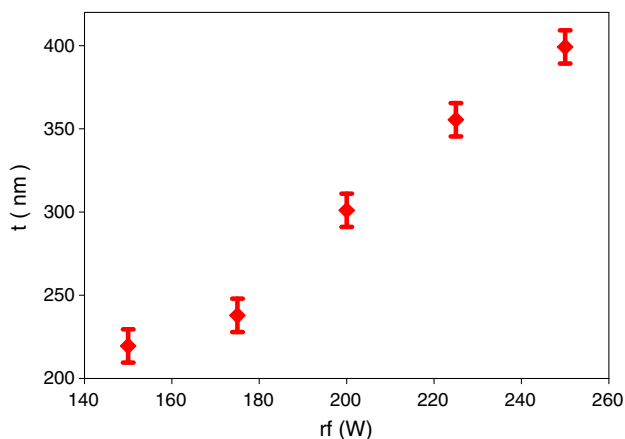


Figure 1 Thickness of the ZnO films on Si substrates as a function of the RF power.

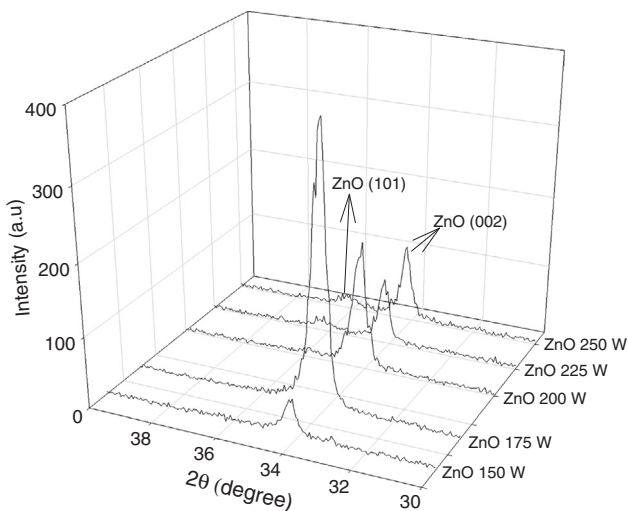


Figure 2 XRD spectra of ZnO films on Si substrates prepared at various RF powers.

Table 1 X-ray diffraction data summary of 002 peak of ZnO films prepared at different RF powers.

Sample	2θ ($^{\circ}$)	FWHM ($^{\circ}$)	d (\AA)	c (\AA)	strain (ϵ_1)	D (nm)
ZnO 150 W	34.1865	0.246	2.6229	5.2458	0.749	35.3058
ZnO 175 W	34.1442	0.3936	2.6260	5.2521	0.869	22.0636
ZnO 200 W	34.1707	0.2460	2.6241	5.2481	0.794	35.3043
ZnO 225 W	34.1866	0.3444	2.6229	5.2458	0.749	25.2184
ZnO 250 W	34.2324	0.2952	2.6195	5.239	0.618	29.4251

Table 2 EDX analysis of ZnO films prepared at different RF powers.

Sample	O K (at.%)	Zn L (at.%)	O/Zn ratio
ZnO 150 W	52.27	47.73	1.10 ± 0.18
ZnO 175 W	52.70	47.30	1.11 ± 0.2
ZnO 200 W	52.05	47.95	1.09 ± 0.2
ZnO 225 W	51.21	48.69	1.05 ± 0.2
ZnO 250 W	50.54	49.46	1.02 ± 0.2

The optical properties of ZnO thin films were investigated by high-spatial resolution photoluminescence (PL), UV-visible spectrophotometer and Raman spectrometer. The Filmetrics F20 unit was used to determine the thickness of the prepared

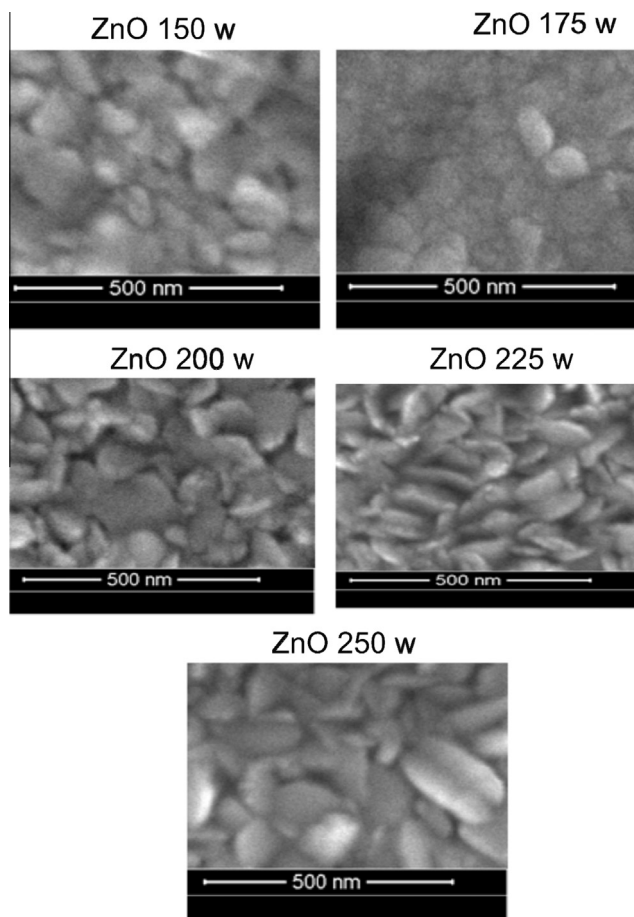


Figure 3 FESEM and AFM images of ZnO films on Si substrates prepared at various RF powers.

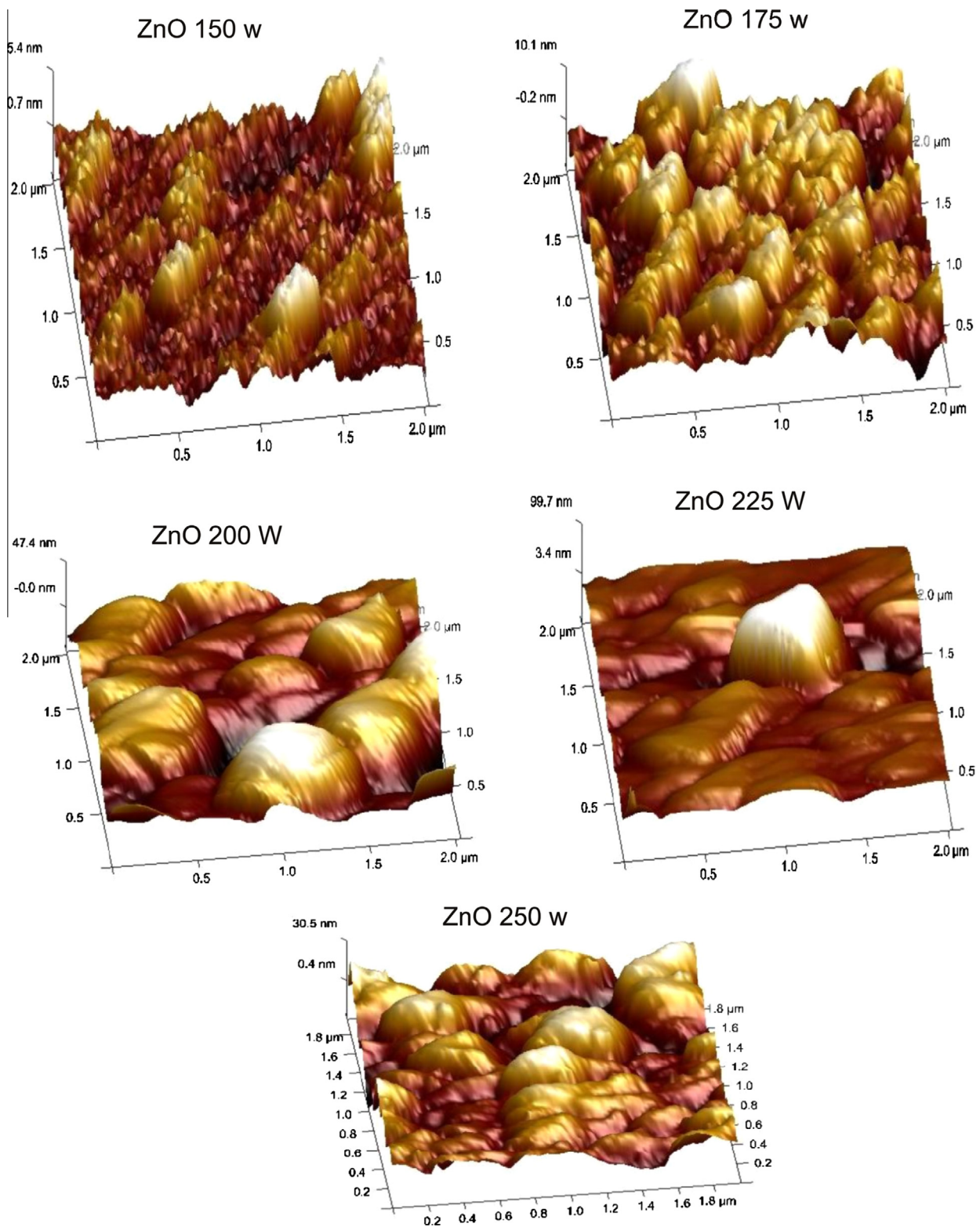


Figure 3 (continued)

films. X-ray diffractometer (source Cu K_{α} with $\lambda = 0.15406$ nm) was used to characterize the structural properties of the ZnO thin films. The surface morphology of the film was determined using AFM and FESEM.

3. Results and discussion

Fig. 1 shows the increased thickness (t) of the prepared films with the increasing RF powers, indicating the proportionality

of the number of atoms sputtered from the target to the applied RF power.

Fig. 2 shows the XRD spectra for the prepared ZnO films from which the (002) peak of ZnO was observed for all the films. For films deposited at 200 W, 225 W and 250 W, (101) peak of ZnO was observed and its intensity increased with the increased RF power. However, for all the films the intensity of (002) peaks was higher as compared to the intensity of (101) peaks indicating that all the films were preferentially *c*-axis oriented. Furthermore, the (002) peaks were reduced for the RF power higher than 175 W indicating less favorable of (002) film orientation suggesting that the increase of RF power induced faster reaction rate that caused insufficient time for the formation of the initially preferred film orientation.

The full width at half maximum (FWHM) of the diffraction peak can be used to estimate the crystallite size (*D*) in the grown films using Scherrer's formula:

$$D = (0.94\lambda) / (\text{FWHM} \cos \theta) \quad (1)$$

The (002) peak was used to estimate the crystallite size, since it is the most intense, and it appeared in all the samples. Table 1 shows the change in FWHM of (002) peaks and the crystallite size with the changing RF powers. The strain along the *c*-axis (ε_1) was estimated using the following equation (Daniel et al., 2010):

$$\varepsilon_1 = [(d_{\text{film}} - d_{\text{powder}}) / d_{\text{powder}}] \times 100 \quad (2)$$

where d_{film} the *d*-spacing for ZnO films and d_{powder} the *d*-spacing for ZnO powder. The variation of *d*-spacing for ZnO films and the strain along the *c*-axis (ε_1) on the changing RF powers are shown in Table 1. The value of *d*-spacing for ZnO films obtained was higher than that of the *d*-spacing for ZnO powder (equal to 0.2604 nm [JCPDS No. 36-1451]), suggesting that all the ZnO films exhibited tensile strain, which is in agreement with the result of Hong et al. (2005).

Table 2 shows the increase of zinc (in %) with increasing RF power from 175 W to 250 W. While at the same time, the presence of oxygen (in %) tends to decrease. Thus, the O:Zn ratio in the film decreased with increasing RF power.

The surface morphology of the films was characterized by AFM and FESEM (Fig. 3) which resulted in the root mean square (rms) of 2.01 nm, 2.81 nm, 7.25 nm, 12.20 nm and 14.83 nm for films prepared at RF powers of 150 W, 175 W, 200 W, 225 W and 250 W, respectively meaning that the root mean square (rms) increased with the increased thickness (*t*) of the prepared films. It was also observed that the shape of the grain changed from round to plate like as the RF power increased. The grain size changes randomly with increasing RF power, which agrees well with the XRD analysis.

Fig. 4 shows the transmittance spectra of the ZnO films, which revealed a good optical transmittance of above 70% in the visible range (380–780 nm). The absorption coefficient (α) determined from the transmittance spectra is related to the photon energy (*E*) as given by:

$$\alpha E = A(E - E_g)^{1/2} \quad (3)$$

where E_g is the energy band gap of the semiconductor and *A* is a constant. Therefore a plot of $(\alpha E)^2$ versus photon energy *E* produced a straight line that cut the photon energy axis at the energy band gap value.

Fig. 5 shows the plot of $(\alpha E)^2$ versus *E* for the prepared samples which produced values of energy band gap of

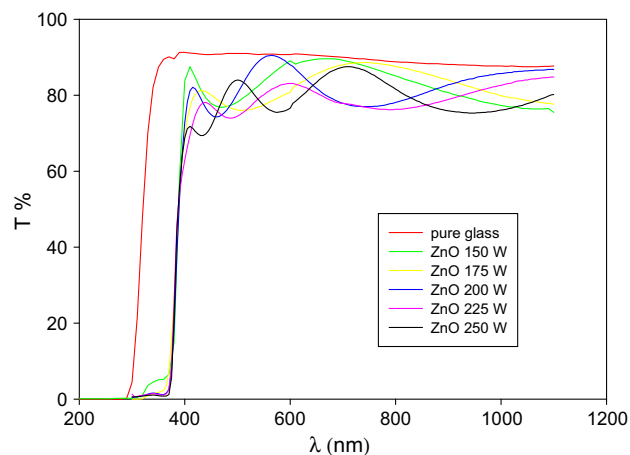


Figure 4 Transmittance spectra of the prepared ZnO thin films on glass substrates with different RF powers.

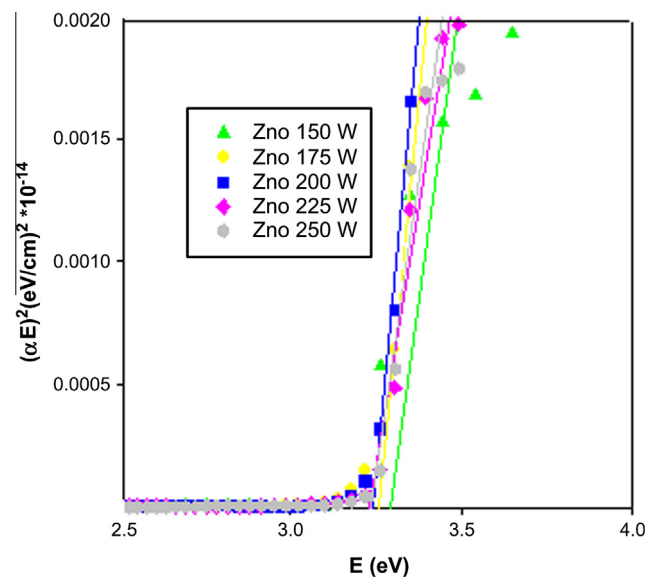


Figure 5 Photon energy (*E*) versus $(\alpha E)^2$ for ZnO thin films on glass substrates prepared at various RF powers.

Table 3 Energy band gap (E_g) and position of UV emission peak at different RF powers of the samples.

Sample	E_g (eV)	Position of UV emission peak (eV)
ZnO 150 W	3.29	3.17
ZnO 175 W	3.26	3.26
ZnO 200 W	3.25	3.28
ZnO 225 W	3.23	3.27
ZnO 250 W	3.24	3.31

3.29 eV, 3.26 eV, 3.25 eV, 3.23 eV and 3.24 eV for films prepared at RF powers of 150 W, 175 W, 200 W, 225 W and 250 W, respectively. Thus, the energy band gap was decreased

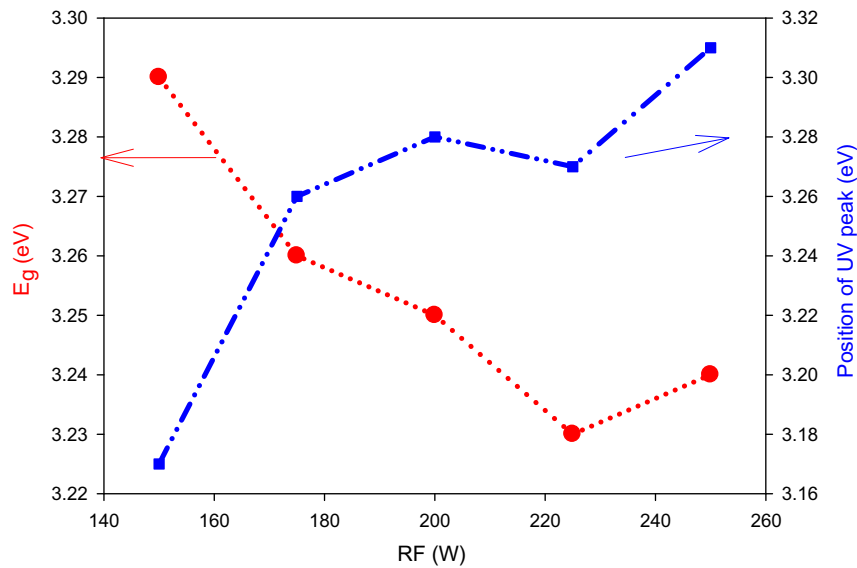


Figure 6 Energy band gap (E_g) and position of UV emission peak as a function of the RF power.

Table 4 Refractive index n (at 550 nm, 600 nm, 700 nm and 800 nm) of ZnO films on Si substrates prepared at various RF powers.

Sample	Refractive index (n at 550 nm)	Refractive index (n at 600 nm)	Refractive index (n at 700 nm)	Refractive index (n at 800 nm)
ZnO 150 W	1.901	1.850	1.864	1.883
ZnO 175 W	1.964	1.891	1.856	1.856
ZnO 200 W	1.928	1.937	1.946	1.946
ZnO 225 W	2.009	1.991	1.973	1.991
ZnO 250 W	2.036	1.982	1.991	2.018

with increasing RF powers with the values close to that of the published values of ZnO (Daniel et al., 2010; Al-Hardan et al., 2010) (Table 3 and Fig. 6).

The refractive index n was calculated by the envelope method using the following equations (Al-Hardan et al., 2010).

$$n = \left[N + (N^2 - n_s^2)^{1/2} \right]^{1/2} \quad (4)$$

$$N = [2n_s(T_M - T_m)/T_M T_m] + (n_s^2 + 1)/2 \quad (5)$$

where T_M and T_m are maxima and minima transmittance and n_s is the refractive index of substrate. The values of n (at 550 nm, 600 nm, 700 nm and 800 nm) obtained are shown in Table 4, which exhibited a tendency to increase with increasing RF powers (Fig. 7).

The photoluminescence (PL) characteristics of the prepared ZnO thin films were obtained at room temperature in the photon energy range 1.24–4.1 eV. All the samples showed UV emission peaks as shown in Fig. 8(a). It was suggested that these peaks were attributed to the free excitons recombination and the strong UV emission in the PL spectra was an indication of a good crystalline structure of the film with excellent optical properties (Zhang et al., 2009). The observed UV emission appeared to be shifted toward higher energy (blue shift) with increasing RF power (Table 3 and Fig. 6). In addition, the observed weak green emission peak (2.36–2.46 eV) shown in Fig. 8(b) for ZnO (225 W) sample is ascribed to the oxygen vacancies (Lai and Lee, 2008).

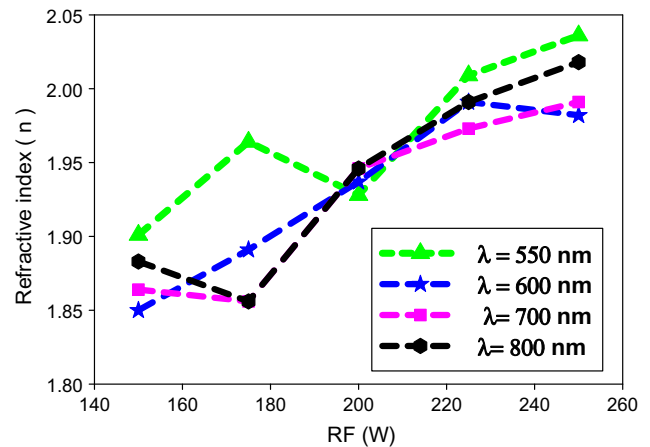


Figure 7 Refractive index n (at 550 nm, 600 nm, 700 nm and 800 nm) of ZnO films on Si substrates prepared at various RF powers.

Fig. 9 shows the Raman spectra of the prepared ZnO thin films where the Raman lines around 433.26 cm^{-1} and 573.72 cm^{-1} were observed for all the samples. These lines were assigned to ZnO E_2 (high) and A_1 longitudinal optical (LO) mode respectively (Cao and Du, 2007). The shift from

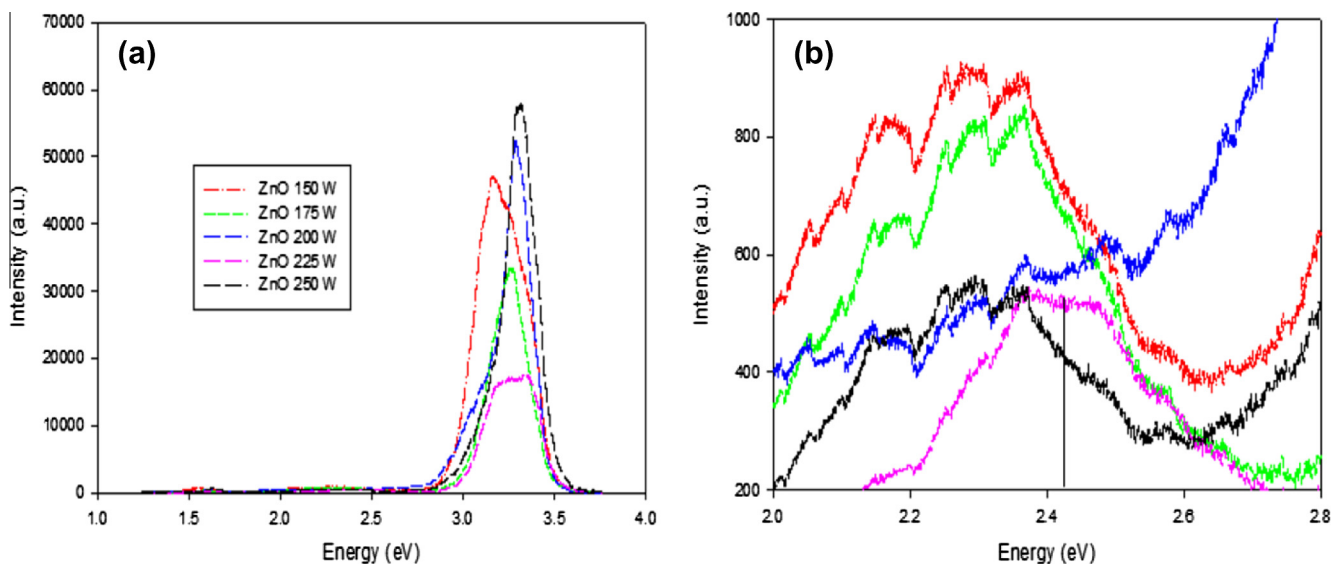


Figure 8 The effect of RF power on the PL spectra of ZnO thin films on Si substrates measured at room temperature.

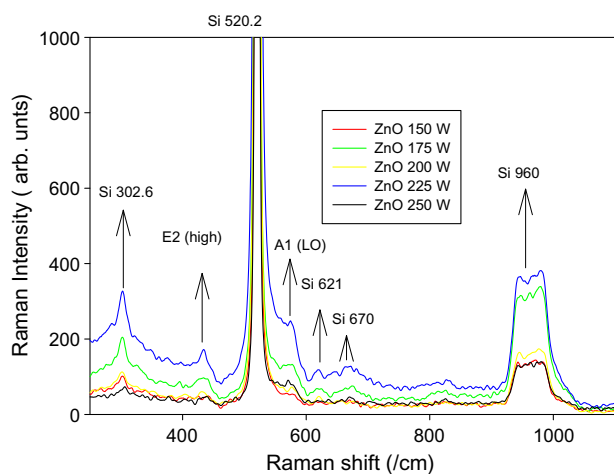


Figure 9 The effect of RF power on the Raman spectra of ZnO thin films on Si substrates measured at room temperature.

437 cm^{-1} to 433.26 cm^{-1} of E_2 (high) was caused by the tensile strain in the films which was in good agreement with the XRD result (Ashkenov et al., 2003). The A_1 (LO) mode was caused by the defects of O-vacancy and Zn interstitial. The increase of the A_1 (LO) intensity for ZnO thin film prepared at RF (225 W) implied the increase of defects (O- vacancy and Zn interstitial) in this film which is consistent with the PL result of Fig. 8(b).

4. Conclusion

The effect of RF power on the structural and optical properties of sputtered ZnO thin films was investigated. XRD results revealed that all the ZnO films were dominantly grown in the c -axis orientation of wurtzite structure. The increase of the RF power (above 175 W) tends to reduce the tensile strain in the film. The observed UV emission peak revealed a blue shift with increasing RF power of the sample. The tensile strain in the

films that caused the Raman lines shift was in good agreement with that obtained from the XRD result. The peak attributed to the oxygen vacancy defect in Raman spectra is consistent with that observed from PL spectra. The optical energy band gap decreased while the refractive index increased as the RF power of the sample increased.

Acknowledgements

This work was partly supported by a short term grant from the Universiti Sains Malaysia.

References

- Al-Hardan, N.H., Abdullah, M.J., et al., 2010. The effect of oxygen ratio on the crystallography and optical emission properties of reactive RF sputtered ZnO films. *Physica B* 405 (4), 1081–1085.
- Alivov, Y.I., Kalinina, E.V., et al., 2003. Fabrication and characterization of n-ZnO/p-AlGaIn heterojunction light-emitting diodes on 6H-SiC substrates. *Appl. Phys. Lett.* 83 (23), 4719–4721.
- Ashkenov, N., Mbenkum, B.N., et al., 2003. Infrared dielectric functions and phonon modes of high-quality ZnO films. *J. Appl. Phys.* 93 (1), 126.
- Cao, W., Du, W., 2007. Strong exciton emission from ZnO microcrystal formed by continuous 532 nm laser irradiation. *J. Lumin.* 124 (2), 260–264.
- Chen, M. et al., 2011. High-sensitivity NO₂ gas sensors based on flower-like and tube-like ZnO nanomaterials. *Sens. Actuators, B* 157 (2), 565–574.
- Daniel, G.P., Justinivictor, V.B., et al., 2010. Effect of annealing temperature on the structural and optical properties of ZnO thin films prepared by RF magnetron sputtering. *Physica B* 405 (7), 1782–1786.
- Hong, R., Qi, H., et al., 2005. Influence of oxygen partial pressure on the structure and photoluminescence of direct current reactive magnetron sputtering ZnO thin films. *Thin Solid Films* 473 (1), 58–62.
- Lai, L.W., Lee, C.T., 2008. Investigation of optical and electrical properties of ZnO thin films. *Mater. Chem. Phys.* 110, 393–396.
- Lau, S.P., Yang, H.Y., et al., 2005. Laser action in ZnO nanoneedles selectively grown on silicon and plastic substrates. *Appl. Phys. Lett.* 87 (1), 013104.

- Li, B.S., Liu, Y.C., et al., 2002. High quality ZnO thin films grown by plasma enhanced chemical vapor deposition. *J. Appl. Phys.* 91 (1), 501.
- Ohgaki, T., Ohashi, N., et al., 2003. Growth condition dependence of morphology and electric properties of ZnO films on sapphire substrates prepared by molecular beam epitaxy. *J. Appl. Phys.* 93 (4), 1961.
- Ozgur, U., Alivov, Y.I., et al., 2005. A comprehensive review of ZnO materials and devices. *J. Appl. Phys.* 98 (4), 041301-103.
- Qiao, Q. et al., 2012. Light-emitting diodes fabricated from small-size ZnO quantum dots. *Mater. Lett.* 74, 104–106.
- Rusu, G.G., Girtan, Mihaela, et al., 2007. Preparation and characterization of ZnO thin films prepared by thermal oxidation of evaporated Zn thin films. *Superlattices Microstruct.* 42 (1–6), 116–122.
- Ryu, Y.R., Zhu, S., 2000. Optical and structural properties of ZnO films deposited on GaAs by pulsed laser deposition. *J. Appl. Phys.* 88 (1), 201.
- Singh, P. et al., 2012. Pulse-like highly selective gas sensors based on ZnO nanostructures synthesized by a chemical route: effect of in doping and Pd loading. *Sens. Actuators, B* 166–167, 678–684.
- Sun, J. et al., 2011. Ultraviolet electroluminescence from ZnO-based light-emitting diode with p-ZnO:N/n-GaN:Si heterojunction structure. *J. Lumin.* 131 (4), 825–828.
- Zhang, R., Yin, P.-G., et al., 2009. Photoluminescence and Raman scattering of ZnO nanorods. *Solid State Sci.* 11 (4), 865–869.